Downloaded from orbit.dtu.dk on: Apr 26, 2025

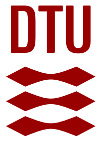

DTU Library

A simple analysis of the stable field profile in the supercritical TEA

Jeppesen, Palle; Jeppsson, B.

Published in:
I E E E Transactions on Electron Devices

Publication date:
1973

Document Version
Publisher's PDF, also known as Version of record

Link back to DTU Orbit

Citation (APA):
Jeppesen, P., & Jeppsson, B. (1973). A simple analysis of the stable field profile in the supercritical TEA. *I E E E Transactions on Electron Devices*, *20*(4), 371-379.

General rights
Copyright and moral rights for the publications made accessible in the public portal are retained by the authors and/or other copyright owners and it is a condition of accessing publications that users recognise and abide by the legal requirements associated with these rights.

- Users may download and print one copy of any publication from the public portal for the purpose of private study or research.
- You may not further distribute the material or use it for any profit-making activity or commercial gain
- You may freely distribute the URL identifying the publication in the public portal

If you believe that this document breaches copyright please contact us providing details, and we will remove access to the work immediately and investigate your claim.

A Simple Analysis of the Stable Field Profile in the Supercritical TEA

PALLE JEPPESEN AND BERT I. JEPPSSON

Abstract—An analytical investigation supported by numerical calculations has been performed of the stable field profile in a supercritical diffusion-stabilized n-GaAs transferred electron amplifier (TEA) with ohmic contacts. In the numerical analysis, the field profile is determined by solving the steady-state continuity and Poisson equations. The diffusion-induced short-circuit stability is checked by performing time-domain computer simulations under constant voltage conditions. The analytical analysis based on simplifying assumptions gives the following results in good agreement with the numerical results. 1) A minimum doping level required for stability exists, which is inversely proportional to the field-independent diffusion coefficient assumed in the simple analysis. 2) The dc current is bias independent and below the threshold value, and the current drop ratio increases slowly and almost linearly with the doping level. 3) The domain width normalized to the diode length L varies almost linearly with $(V_B/V_T-1)^{\frac{1}{2}}/(n_0L)^{\frac{1}{2}}$, where V_B is the bias voltage, V_T is the threshold voltage, and n_0 is the doping level. 4) The peak domain field varies almost linearly with $(V_B/V_T-1)^{\frac{1}{2}}(n_0L)^{\frac{1}{2}}$. Those results contribute to the understanding of the high n_0L-product switch and the stability of the supercritical TEA.

I. Introduction

THIS PAPER presents a numerical, and in particular an analytical, analysis of the stable high-field domain in the anode of a supercritical diffusion-stabilized n-GaAs transferred electron device (TED) with ohmic contacts [1].

Stable anode domains were first discovered in probing experiments by Thim and Knight [2], and then observed experimentally and in computer simulations by Shaw *et al.* [3] for cathode fields below the threshold field for onset of negative differential mobility. Stable anode domains were also observed in computer simulations by Magarshack and Mircea [4], [5], who furthermore predicted a bandwidth exceeding one octave for the negative resistance of diffusion-stabilized TED's. In such devices, bistable switching—made possible by the presence of stable anode domains—has been observed by Thim [6] and Boccon-Gibod and Teszner [7]. Moreover, a small-signal analysis of Guéret [8] has led to the following criterion for a diffusion-dominated anode nonuniformity to nucleate a stationary high-field layer:

$$\tau_1 < \frac{2}{v} L_D = \frac{2}{v}\sqrt{D\tau_1}. \tag{1}$$

Here τ_1 is the numerical value of the negative dielectric relaxation time, L_D is the Debye length, D is the diffusion coefficient, and v is the electron drift velocity. This criterion for absolute instability [8] suggests that the stationary anode layer should appear for doping levels exceeding a diffusion-dependent lower limit. This conclusion agrees with time-domain computer studies by Thim [9] and by Guéret and Reiser [10], in which switching to a low-current stable state with anode-layer formation takes place for doping levels above a lower limit given approximately by criterion (1). Thim [9] derived this criterion heuristically by requiring that the accumulation layer should readjust more quickly than it moves into the anode. Along the same line of thought, the authors [11] have also performed computer simulations in which the response of a diode to a quickly applied bias voltage has been studied. Ohmic contacts and a homogeneous doping profile were assumed for the diode. Provided the field-dependent diffusion coefficient was sufficiently large, a gradual decay in the peak of the accumulation layer for each passage into the anode was observed, until the final stable field configuration with a high-field domain in the anode was reached. This stable field configuration was possible because the diffusion current helped preserve the current continuity in the accumulation layer associated with the anode domain. During the decay of the current, transient accumulation layer transits—as opposed to domain transits—were observed [11] because ohmic contacts imply low cathode fields, which in turn assure that the cathode is not a major domain nucleation site. For nonohmic cathodes with cathode fields well in the range between the threshold and valley field of the velocity–field characteristic, transit-time Gunn domain oscillations will occur [3] without any stable solution. However, for cathode fields only slightly above threshold, stable anode domains is still a possible solution [3], [12].

The present simple analysis explains why the diffusion coefficient must be sufficiently large, why there is a diffusion-dependent lower limit for the doping level, why the device switches to a high-voltage state with saturated current, and how the stable field con-

Manuscript received September 14, 1972; revised October 30, 1972. This work was supported in part by the Reinholdt W. Jorck Foundation.
P. Jeppesen is with the Laboratory of Electromagnetic Theory, Technical University of Denmark, Lyngby, Denmark.
B. I. Jeppsson is with the Microwave Department, Royal Institute of Technology, Stockholm, Sweden.

figuration depends on doping level and applied bias. Such an analysis is felt to be of interest because it contributes to the understanding of the supercritical transferred electron amplifier and the bistable switch.

The stable field configuration is investigated by considering the Poisson and the current continuity equations. Even for a piecewise linearized velocity–field characteristic and a field-independent diffusion coefficient, the direct solution of those two fundamental equations is not very practical. However, by also assuming a linear variation for the electron density versus distance in the upstream portion of the domain, a simple and useful approximate solution is easily obtained.

In Section II the numerical investigation is described before the simplifying assumptions used in the simple analysis are introduced, and then formulas for later use are derived. Section III deals with a simple limiting case, which serves the purpose of emphasizing the physics involved. Proceeding from the simple to the more complicated case, Section IV treats the general case, for which the bias current, the width, and the peak field of the domain are calculated as functions of bias voltage, doping level, and diode length. The results are shown to be in good agreement with numerical solutions. Section V contains concluding remarks.

II. Formulation of the Model

Before a simple analytical model is formulated, it is useful to summarize the numerical calculations and results.

A. Numerical Results

The question of stability and the eventual stable field profile was first investigated by solving numerically the time-dependent problem. With reference to the sign convention of Fig. 1(a), the fundamental equations in the active layer of the diode are the Poisson equation

$$\frac{\partial E}{\partial x} = \frac{q}{\epsilon}(n - n_0) \tag{2}$$

and the continuity equation

$$J(t) = qnv - q\frac{\partial}{\partial x}(Dn) + \epsilon\frac{\partial E}{\partial t} \tag{3}$$

where $E(x, t)$ is the space- and time-dependent electric field, $n(x, t)$ is the free-electron density, n_0 is the net donor density in the active layer, $-q(q>0)$ is the electric charge, ϵ is the absolute permittivity of GaAs, $J(t)$ is the space-independent total current density, $v(E)$ is the electron drift velocity–electric field characteristic, and $D(E)$ is the electron diffusion coefficient-electric field characteristic suggested by Copeland [13]. The $v(E)$- and $D(E)$-characteristics are shown in Fig. 1(b) and (c), respectively. The numerical solution of (2) and (3) under constant voltage conditions and using

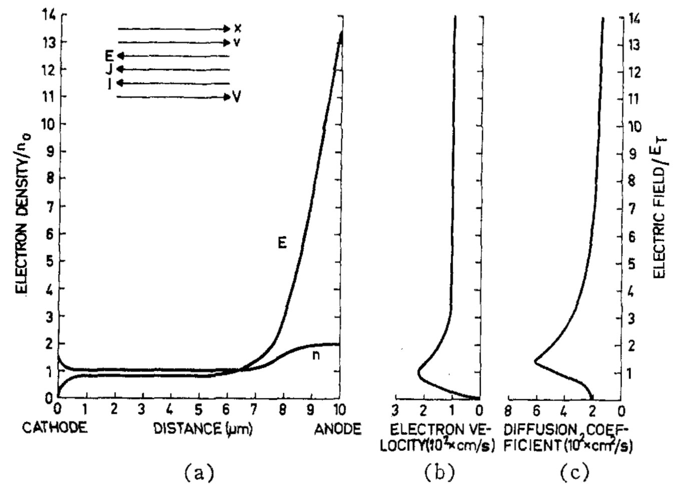

Fig. 1. (a) Normalized electric field E/E_T and electron density n/n_0 versus distance for computer simulation. (b) Electron drift velocity—electric field characteristic. (c) Diffusion coefficient—electric field characteristic. Diode data: $L=10$ μm, $n_0=1.5\times10^{15}$ cm^{-3}, $E_T=3.48$ kV/cm, $V_B/V_T=2.74$, $T_0=300$ K.

boundary conditions relevant to heavily doped ohmic contacts is obtained using a finite difference method. The bias voltage was quickly applied to the diode, and then the decay of the induced large-signal transient was studied as the domain reached its stable state after several accumulation layer transits [11]. As only constant voltage conditions are considered, a stable solution represents short-circuit stability. In the following, stability is therefore referred to as short-circuit stability, leaving open the question of open-circuit stability or more complicated circuit-controlled stabilities.

In the following, a diode having the active layer length $L=10$ μm and the lattice temperature $T_0=300$ K was chosen. For a field-independent diffusion coefficient $D_0=200$ cm²/s replacing the $D(E)$- characteristic of Fig. 1(c) short-circuit stability with a high-field domain in the anode was found for $n_0>2\times10^{15}$ cm^{-3} [5]. When D_0 was increased to 400 cm²/s, short-circuit stability existed for doping levels down to 1×10^{15} cm^{-3}, and for 500 cm²/s down to the subcritically doped range where the device also is short-circuit stable [14], although the stability in this range does not stem from diffusion effects. For the $D(E)$-characteristic of Fig. 1(c), short-circuit stability was also found down to the subcritical doping range, although the stability was marginal around 5×10^{14} cm^{-3}.

Having settled the question of short-circuit stability, the stable field profile was then studied for various bias and doping levels. To this end, the steady-state (time-independent) equations were used, so that computer time could be saved by not having to calculate through sometimes slowly decaying transients. Now the Poisson equation writes

$$\frac{dE}{dx} = \frac{q}{\epsilon}(n - n_0) \tag{4}$$

and the continuity equation

$$J = qnv - q \frac{d}{dx}(Dn). \quad (5)$$

The numerical solution of those two equations is obtained using an iterative method. In cases where the device is short-circuit stable, the time-dependent and steady-state equations give the same solution for identical conditions. A typical stable solution is shown in Fig. 1(a) for $n_0 = 1.5 \times 10^{15}$ cm^{-3} and for the bias voltage $V_B = 2.74 \times V_T$, where $V_T = LE_T$ is the threshold voltage and $E_T = 3.48$ kV/cm is the threshold field.

The numerical procedure can easily tackle the nonlinear problem, but it does not provide an interpretation of the solution in simple physical terms. Therefore, (4) and (5) will be treated analytically in the following by introducing suitable simplifying assumptions.

B. *The Piecewise Linear $v(E)$-Characteristic*

In Fig. 2(a) the electric field and electron density profiles are shown schematically in relation to a piecewise linear $v(E)$- characteristic [Fig. 2(b)] given by

$$v = \begin{cases} \mu_0 E \quad \text{for } 0 \leqq E < E_T & (6) \\ v_T - \mu_1(E - E_T) \quad \text{for } E_T \leqq E < E_V & (7) \\ v_V \quad \text{for } E_V \leqq E < \infty \end{cases}$$

where the threshold velocity v_T, valley velocity v_V, threshold field E_T, valley field E_V, low-field mobility μ_0, and negative differential mobility $-\mu_1(\mu_1 > 0)$ are related according to

$$v_T = \mu_0 E_T \quad (8)$$

and

$$\mu_1 = \frac{v_T - v_V}{E_V - E_T}. \quad (9)$$

In the numerical examples to be discussed later, the following data for the $v(E)$- characteristic will be used: $E_T = 3.48$ kV/cm, $E_V/E_T = 2.5$, $v_V = 10^7$ cm/s, the velocity peak-to-valley ratio $v_T/v_V = 2.2$, and $\mu_0 = 6310$ cm^2/V·s and $\mu_1 = 2300$ cm^2/V·s according to (8) and (9), respectively. These values approximate the input data used in the numerical calculations.

C. *The Diffusion Coefficient*

In this simple analysis, no attempt will be made to fully treat consequences that might stem from the field dependence of the diffusion coefficient. For simplicity, a field-independent coefficient D_0 will be used instead. The Copeland diffusion curve [Fig. 1(c)] exhibits a peak of 600 cm^2/s for fields slightly above threshold. As the diffusion level, particularly in this field range, affects the field profile and thereby the stability, the Copeland curve will in the following simple analysis be approximated by the field-dependent $D_0 = 500$ cm^2/s, and the consequences of assuming smaller D_0 values also will discussed.

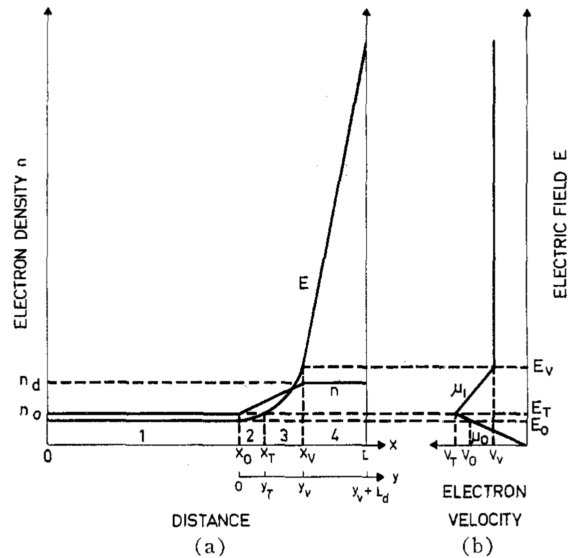

Fig. 2. (a) Piecewise linear electron density and electric field profiles. (b) Piecewise linear electron drift velocity—electric field characteristic.

D. *The Subsections of the Diode*

With reference to Fig. 2(a) and keeping Fig. 1(a) in mind, the length of the diode is divided into four regions. Region 1 is defined by $0 \leqq x < x_0$, where x_0 is the x value, where E becomes greater than the field in front of the domain E_0, and n greater than n_0. Region 2 is defined by $x_0 \leqq x < x_T$, where x_T is implicitly given by $E(x_T) = E_T$. Region 3 is defined by $x_T \leqq x < x_V$, where x_V is implicitly given by $E(x_V) = E_V$. Region 4 is defined by $x_V \leqq x < L = x_V + L_d$, where L_d is the width of the part of the domain, where $E \geqq E_V$.

In region 1, the continuity equation (5) writes $J = qn_0v_0$, where $v_0 = \mu_0 E_0$. The field E_0 determines the current density, and is therefore an unknown of main interest. It should be pointed out that $E_0 \leqq E_T$ is assumed, in agreement with computer results [Fig. 1(a)] and bistable switching experiments [6] and [7], where a current density lower than the threshold value $J_T = qn_0v_T$ is encountered.

In region 2, both the electron density and the electric field increase towards the anode. According to the equation

$$n_0 v_0 = nv - D_0 \frac{dn}{dx}, \quad (10)$$

current continuity can only be preserved provided the diffusion term $D_0(dn/dx)$ is sufficiently large. This conclusion is of crucial importance and shall be investigated further.

In region 3, E is steadily increasing with x, and v is therefore steadily decreasing. Moreover, n is increasing with x, and any variation in the conduction term nv

must be balanced by the diffusion term. Note that according to (10), the current continuity would be violated if n was constant in any range of region 3.

Finally, in region 4, E increases from E_V to the peak domain field E_d and v remains constant at v_V. The corresponding variation in n can be obtained from

$$n_0 v_0 = n v_V - D_0 \frac{dn}{dx},$$

which can be integrated to

$$n(x) = [n(x_V) - n_d] \exp\left[\frac{v_V}{D_0}(x - x_V)\right] + n_d$$

where

$$n_d = n_0 \frac{v_0}{v_V}. \qquad (11)$$

In the exponential function, typical values are $v_V = 10^7$ cm/s, $D_0 = 500$ cm^2/s, and, for example, $x - x_V = 2$ μm, giving $v_V(x - x_V)/D_0 = 4.0$. This represents such a strong variation in n that in order to comply with the numerical solution, it is necessary to require that $n(x_V) = n_d$, which leads to $n(x) = n_d$ for $x_V \leqq x < L$.

It is now important to make the following conclusion. As $n(x)$ remains constant at n_d in region 4, and is steadily increasing in region 3, continuity in $n(x)$ requires that $n(x)$ must exactly reach n_d at the interface where by definition $E = E_V$. This observation provides the final equation needed to determine the stable field profile.

Finally, (11) also shows that since v_0 is upper bounded by v_T, n_d must be upwards limited by $n_{d,\max} = n_0\, v_T/v_V$.

E. The Linear Electron Density Assumption

For simplicity we introduce the substitution $y = x - x_0$, into which x_T and x_V are substituted in order to define the useful parameters $y_T = x_T - x_0$ and $y_V = x_V - x_0$ [Fig. 2(a)].

Even using the simplified $v(E)$- characteristic and the diffusion coefficient D_0 introduced so far, an exact integration of (4) and (5) is cumbersome, if at all possible. Instead, the current continuity equation (10) will be integrated from $y = 0$ to $y = y_V$:

$$n_0 v_0 y_V = \int_0^{y_V} n v dy - D_0(n_d - n_0). \qquad (12)$$

As shown in Fig. 1(a), the numerical solution gives an almost linear variation for $n(x)$ in regions 2 and 3. Therefore, little error is introduced when evaluating the integral in (12) by assuming the linear variation

$$n = n_0 + \frac{n_d - n_0}{y_V} y, \qquad 0 \leqq y \leqq y_V. \qquad (13)$$

Using this assumption, expressions for y_V and y_T are derived in Appendix A.

III. The Limiting Case

In order to emphasize the simple physical idea underlying the mathematical treatment, this section is devoted to a simple case being at the verge of instability because the field in front of the domain equals the threshold field for negative differential mobility. For this situation, which occurs, for example, for a sufficiently small diffusion coefficient, the concept of minimum diffusion and doping density required for stability is introduced.

A. Minimum Diffusion Required for Stability

As summarized in a previous publication [11], controversy evidently surrounds the $D(E)$- characteristic in GaAs. It was also shown in this publication that a field-independent diffusion coefficient had to exceed a certain doping-dependent lower limit in order to attain the diffusion-stabilized condition.

With reference to Fig. 2, let us imagine that the field-independent D_0 is decreased while n_0 is kept fixed. For a smaller D_0, $n(x)$ will vary more abruptly versus distance in regions 2 and 3, which means that y_V will decrease. Now, the Poisson equation (4) can be integrated to

$$E_V = \frac{v_0}{\mu_0} + \frac{q}{\epsilon}\int_0^{y_V} (n - n_0)\, dy$$

where, for the moment, v_0 and $n(y_V) = n_0 v_0 / v_V$ will be thought of as being functions of y_V. The differentiation with respect to y_V gives

$$\frac{dv_0}{dy_V} + \frac{q n_0 \mu_0}{\epsilon v_V} v_0 = \frac{q n_0 \mu_0}{\epsilon},$$

which is easily integrated to

$$v_0 = v_V + (v_T - v_V) \exp\left[-\frac{q n_0 \mu_0}{\epsilon v_V}(y_V - y_{V,\min})\right] \qquad (14)$$

using the boundary condition $v_0(y_{V,\min}) = v_T$. Equation (14) shows that when D_0 and thereby y_V decreases, v_0 increases towards its upper limit v_T. Simultaneously, E_0 reaches E_T, which for a uniform doping profile is the limit for stability. This situation is called the limiting case.

B. The Minimum Diffusion Coefficient for Stability

Equation (14) serves the purpose of showing that v_0 will increase as progressively smaller D_0 values are considered. However, the minimum diffusion coefficient for stability $D_{0,\min}$, for which $v_0 = v_T$, cannot be determined from this equation. Instead (12) is considered in the form

$$n_0 v_T y_{V,\min} = \int_0^{y_{V,\min}} n v dy - D_{0,\min}(n_{d,\max} - n_0), \qquad (15)$$

which, as outlined in Appendix B, leads to

$$D_{0,\min} = \frac{\epsilon v_V^2}{q\mu_1 n_0}\left(\frac{1}{2}\frac{v_T}{v_V} - \frac{1}{6}\right). \tag{16}$$

This result will be discussed further in the broader context of Section IV-B.

IV. The General Case

From the simple limiting case, we shall now proceed to the general case, where the field in front of the domain is below threshold.

A. The General Case as a First-Order Perturbation

It was shown in Section II-D that in region 1 [Fig. 2(a)] $v_V < v_0 < v_T$, which means that E_0 is not too far below E_T, as also has been observed in numerous computer calculations. Therefore, in the following analysis let

$$E_0 = E_T - \Delta E \tag{17}$$

where $\Delta E \ll E_T$, so that this general case is treated as a first-order perturbation of the limiting case. Accordingly, the velocity v_0 in front of the domain is given by

$$v_0 = v_T - v_T \frac{\Delta E}{E_T}. \tag{18}$$

B. The Minimum Doping Level for Stability

In this section, n_0 will be varied for a fixed D_0 in order to show that a minimum doping level for stability $n_{0,\min}$ exists. To this end, the relative field drop $\Delta E/E_T$ is calculated in a procedure that is similar to the one in Section III-B, since it also is based on (10). According to Appendix C, the relative field drop is given by

$$\frac{\Delta E}{E_T} = \frac{\frac{qD_0n_0}{\epsilon v_V E_T}\left(\frac{v_T}{v_V}-1\right) - \left(\frac{E_V}{E_T}-1\right)\left(\frac{1}{2}\frac{v_T}{v_V}-\frac{1}{6}\right)}{\frac{qD_0n_0}{\epsilon v_V E_T}\frac{v_T}{v_V}+\frac{4}{3}\left(\frac{E_V}{E_T}-1\right)\frac{v_T}{v_T-v_V}+\left(\frac{v_T}{v_V}+\frac{2}{3}\right)}. \tag{19}$$

As shown in Section IV-C, this formula implies that $\Delta E/E_T$ decreases with decreasing n_0. However, in order for the diode to be stable, it is necessary that $\Delta E > 0$, requiring

$$n_0 > n_{0,\min} = \frac{\epsilon v_V E_T}{qD_0} \frac{\frac{E_V}{E_T}-1}{\frac{v_T}{v_V}-1}\left(\frac{1}{2}\frac{v_T}{v_V}-\frac{1}{6}\right),$$

which by use of (9) also can be written

$$n_{0,\min} = \frac{\epsilon v_V^2}{q\mu_1 D_0}\left(\frac{1}{2}\frac{v_T}{v_V}-\frac{1}{6}\right). \tag{20}$$

This expression is identical to (16), in agreement with the fact that the general case has been treated as a first-order perturbation of the limiting case. Substituting into (20) $q = 1.6\times10^{-19}$ C, $\epsilon = 13.2\epsilon_0 = 1.17\times10^{-12}$ F/cm, the data for the $v(E)$-characteristic of Section II-B and $D_0 = 200$ or 400 cm²/s give, respectively, $n_{0,\min} = 1.5\times10^{15}$ or 7.4×10^{14} cm^{-3}. Those values are in good agreement with numerical results [5], [11], which supports the simple analysis. For $D_0 = 500$ cm²/s, the value approximating the Copeland curve, $n_{0,\min} = 5.9\times10^{14}$ cm^{-3} is obtained. This low value is close to the stable subcritical range (for $L = 10$ μm), in agreement with the numerical calculations in Section II-A, where the Copeland diffusion curve led to stability for any doping level of practical interest.

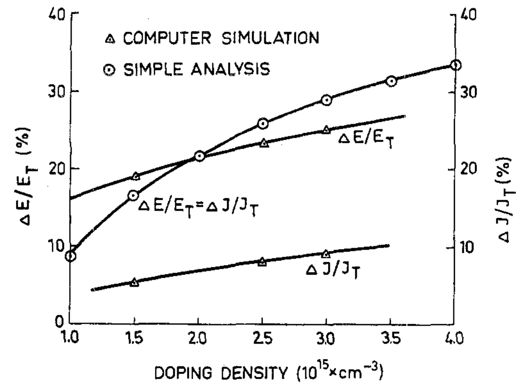

Fig. 3. Relative field drop $\Delta E/E_T$ in front of domain, and relative current density drop $\Delta J/J_T$ versus doping density obtained from simple analysis and computer simulation.

It is interesting to compare (20) with the criterion (1) of Guéret [8], which can be written

$$n_{0,\min} = \frac{\epsilon v^2}{4q\mu_1 D}. \tag{21}$$

The two expressions are quite similar, and (21) yields the same value for $n_{0,\min}$ if a drift velocity close to v_T is substituted for v. A similar expression has been obtained by Thim [9].

C. The Current Density

For the specific example considered earlier with $D_0 = 500$ cm²/s, the relative field drop in front of the domain $\Delta E/E_T$ as calculated from (24) is plotted versus n_0 in Fig. 3. For comparison, the corresponding curve obtained from the numerical calculations in Section II-A is also shown, and good agreement is found. Now in the simple analysis, the dc current density is given by $J = J_T - \Delta J$, where $J_T = qn_0\mu_0E_T$ is the threshold current density and $\Delta J = qn_0\mu_0\Delta E$ is the current density drop, which means in turn that $\Delta J/J_T = \Delta E/E_T$. In the computer simulations, however, the current density drop is somewhat lower than $\Delta E/E_T$, as shown in Fig. 3. This stems from the curvature of the $v(E)$-characteristic around the peak velocity [Fig. 1(b)]. The fact that $\Delta J/J_T$ increases with increasing n_0 means that the bistable switching phenomenon in supercritical TED's

will get more pronounced as the doping level is increased.

For the subcritical amplifier, J increases with increasing bias because of an increasing amount of injected space charge. The diode thus exhibits a positive differential resistance at dc in spite of its negative differential mobility, as predicted by Shockley [15]. However, for the diffusion-stabilized amplifier, (19) predicts a bias-independent dc current. This agrees with published experimental results [1] and with the numerical calculations of Section II-A, in which a bias variation of, for example, a factor of three caused no current variation at all. As recently pointed out in the literature [16], [17], this bias-independent current is not in contradiction with Shockley's positive conductance theorem.

D. The Domain Width

The width of the part of the domain where $E>E_T$ is $L_d+y_V-y_T \simeq L_d+y_V$ since $y_T \ll y_V$ (Fig. 2). This domain width now will be determined.

The width L_d of the part of the domain where $E>E_V$ (Fig. 2) can be found by equating the area below the field profile with the applied bias voltage $V_B=LE_B$, where E_B is defined as the average bias field. This area can naturally be divided into the four hatched areas shown in Fig. 4. Hence,

$$V_B = V_1 + V_2 + V_3 + V_4 \tag{22}$$

where the voltages V_1, V_2, V_3, and V_4 are equal to the four areas, respectively. Those areas are calculated in Appendix D, where the method for obtaining the following formula is also outlined:

$$\frac{L_d}{L} = \sqrt{\frac{2\epsilon E_T}{qn_0L} \frac{\frac{V_B}{V_T}-1}{\frac{v_T}{v_V}-1}} \cdot \left[1+\left(\frac{v_T}{v_T-v_V}+\frac{V_T}{V_B-V_T}\right)\frac{\Delta E}{2E_T}\right]. \tag{23}$$

For $1.5\times10^{12}<n_0L<3.5\times10^{12}$ cm^{-2}, $5>V_B/V_T>2$, $D_0=500$ cm^2/s, and the $v(E)$-characteristic of Section II-B, (23) gives $39>L_d/L>16$ percent.

As far as y_V is concerned, one obtains (to the first order in $\Delta E/E_T$) from (A.4), (11), and (17)

$$\frac{y_V}{L} = \frac{2\epsilon E_T}{qn_0L}\left(\frac{E_V}{E_T}-1\right)\frac{v_V}{v_T-v_V} \cdot \left[1+\left(\frac{v_T}{v_T-v_V}+\frac{E_T}{E_V-E_T}\right)\frac{\Delta E}{2E_T}\right]. \tag{24}$$

For $1.5\times10^{12}<n_0L<3.5\times10^{12}$ cm^{-2}, this equation gives $6.1>y_V/L>3.0$ percent. Therefore, y_V constitutes a minor correction to L_d in the domain width L_d+y_V.

In Fig. 5 the normalized domain width $(L_d+y_V)/L$ versus the normalized bias voltage is plotted for two typical cases $n_0L=1.5\times10^{12}$ and 3.0×10^{12} cm^{-2}. Since $y_V \ll L_d$ and $\Delta E \ll E_T$, the normalized domain width is inversely proportional to $(n_0L)^{1/2}$ and proportional to $(V_B/V_T-1)^{1/2}$. When V_B is increased, the high-field portion of the stable domain moves towards the cathode with constant slope because the dc current is bias independent. For comparison, the numerical curves are also shown, and excellent agreement is found.

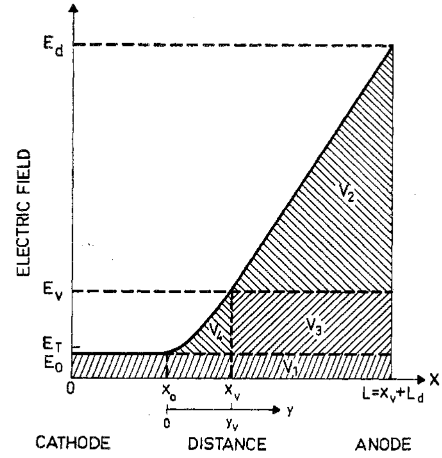

Fig. 4. Bias voltage divided into four parts.

E. The Domain Peak Field

Using L_d values obtained from (23), the peak domain field now will be calculated from (22), written in the form

$$V_B = LE_0 + \tfrac{1}{2}L_d(E_d - E_V) + L_d(E_V - E_0)$$

where the small V_4 has been neglected for simplicity. Solving this equation with respect to E_d, and subsequent substitution of (17) yields

$$\frac{E_d}{E_T} = 2\frac{L}{L_d}\left(\frac{V_B}{V_T}-1+\frac{\Delta E}{E_T}\right)+2-\frac{E_V}{E_T}-2\frac{\Delta E}{E_T},$$

in which substitution of (23) to the first order in $\Delta E/E_T$ gives

$$\frac{E_d}{E_T} = \sqrt{\frac{2qn_0L}{\epsilon E_T}\left(\frac{v_T}{v_V}-1\right)\left(\frac{V_B}{V_T}-1\right)} \cdot \left[1-\left(\frac{v_T}{v_T-v_V}-\frac{V_T}{V_B-V_T}\right)\frac{\Delta E}{2E_T}\right] + 2 - \frac{E_V}{E_T} - 2\frac{\Delta E}{E_T}. \tag{25}$$

The significance of this equation is illustrated in Fig. 6, where E_d/E_T is plotted versus V_B/V_T for the $v(E)$-characteristic, the diffusion coefficient, and the n_0L-products considered earlier. The analytical results are shown to be in good agreement with the numerical results. As seen from (25), E_d/E_T varies almost linearly with $(n_0L)^{1/2}$ and $(V_B/V_T-1)^{1/2}$ because $\Delta E/E_T \ll 1$.

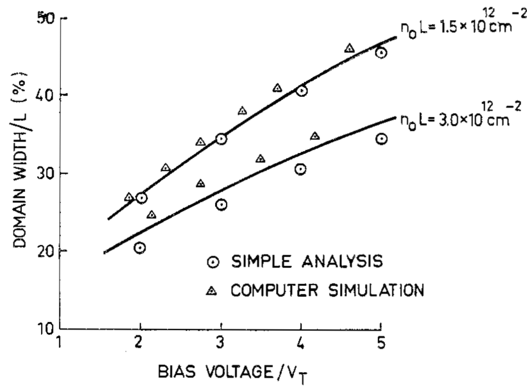

Fig. 5. Normalized domain width versus normalized bias voltage for simple analysis and computer simulation considering two typical n_0 L-products.

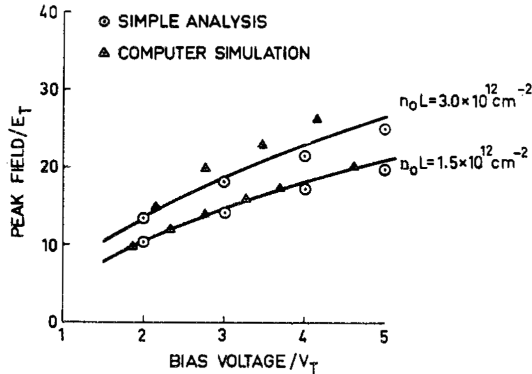

Fig. 6. Normalized peak domain field versus normalized bias voltage for simple analysis and computer simulation considering two typical n_0L-products.

V. Conclusion

An analytical investigation, supported by numerical calculations, of the stable field profile in a diffusion-stabilized TEA with ohmic contacts has been performed. Using the Copeland diffusion curve in the numerical calculations, a 10-μm device was found to be short-circuit stable for any doping range of practical interest. The stability, however, was marginal for doping levels around 5×10^{14} cm^{-3}. Introducing in the analytical investigation a field-independent diffusion coefficient D_0 along with suitable simplifying assumptions for the $v(E)$-characteristic and also for the electron density profile, the conclusions obtained are these.

1) A minimum doping level required for stability exists, which is inversely proportional to the diffusion coefficient assumed for GaAs. For $D_0=500$ cm^2/s, the value chosen to approximate the Copeland diffusion curve, the minimum doping level is 5.9×10^{14} cm^{-3}.

2) In a first-order approximation, the dc current is bias independent and below threshold. The relative current drop varies slowly and almost linearly with the doping level (Fig. 3).

3) The normalized domain width is approximately inversely proportional to $(n_0L)^{1/2}$, and the normalized domain peak field varies almost linearly with $(n_0L)^{1/2}$.

4) The normalized width and peak field of the domain both vary almost linearly with $(V_B/V_T-1)^{1/2}$ because the dc current is bias independent, which forces the domain to keep its slope in electric field constant for varying bias level.

5) The results are in good agreement with detailed numerical results, and thus provide an explanation in simple physical terms of the existence and behavior of stable anode domains.

These conclusions contribute to the understanding of the high n_0L-product bistable switch and the stability of the supercritical TEA.

Appendix A

Calculations of y_v and y_T

From (4) and (13), we get by integration

$$\frac{dE}{dy} = \frac{q}{\epsilon}\,\frac{n_d - n_0}{y_V}\,y, \qquad 0 \leqq y \leqq y_V, \tag{A.1}$$

which is integrated to

$$E = E_0 + \frac{q}{\epsilon}\,\frac{n_d - n_0}{2y_V}\,y^2, \qquad 0 \leqq y \leqq y_V. \tag{A.2}$$

Substitution of $y=y_V$ into this equation gives

$$E_V = E_0 + \frac{q}{\epsilon}\,\frac{n_d - n_0}{2}\,y_V, \tag{A.3}$$

from which y_V can be obtained using (11):

$$y_V = \frac{2\epsilon}{qn_0}\,\frac{v_V}{v_0 - v_V}\,(E_V - E_0). \tag{A.4}$$

Similarly, substitution of $y=y_T$ gives

$$y_T = \frac{2\epsilon}{qn_0}\,\frac{v_V}{v_0 - v_V}\,\sqrt{(E_V - E_0)(E_T - E_0)}. \tag{A.5}$$

Appendix B

Calculation of the Minimum Diffusion Coefficient for Stability

For the limiting case with $E_0=E_T$, formula (A.4) simplifies to

$$y_{V,\min} = \frac{2\epsilon}{qn_0}\,\frac{v_V}{v_T - v_V}\,(E_V - E_T) = 2\tau_1 v_V \tag{B.1}$$

where the negative dielectric relaxation time τ_1 is given by

$$\tau_1 = \frac{\epsilon}{qn_0\mu_1}\,. \tag{B.2}$$

Moreover, y_T obviously vanishes and

$$n_d = n_{d,\max} = n_0\frac{v_T}{v_V}\,. \tag{B.3}$$

The integral in (15) can be evaluated using (4), (7), (A.1), (B.1), (B.3), and (9):

$$\begin{aligned}\int_0^{y_{V,\min}} nv\,dy &= \int_0^{y_{V,\min}} \left(n_0 + \frac{\epsilon}{q}\frac{dE}{dy}\right) v\,dy \\ &= n_0 \int_0^{y_{V,\min}} v\,dy + \frac{\epsilon}{q}\int_{E_T}^{E_V} v\,dE \\ &= n_0\left[yv + \int y\mu_1 \frac{dE}{dy}\,dy\right]_0^{y_{V,\min}} \\ &\quad + \frac{\epsilon}{q}\int_{E_T}^{E_V}[v_T - \mu_1(E - E_T)]\,dE \\ &= n_0 2\tau_1 v_V[v_V + \tfrac{2}{3}(v_T - v_V)] \\ &\quad + \frac{\epsilon}{2q\mu_1}(v_T - v_V)(v_T + v_V). \qquad \text{(B.4)}\end{aligned}$$

This expression for the integral, along with (B.1), (B.3), and (B.2), are then substituted into (15), and when this equation is solved with respect to $D_{0,\min}$, expression (16) is obtained.

Appendix C

Outline of the Calculation of the Relative Field Drop

By using (4), (6), and (7), the integral in (12) can be evaluated as follows:

$$\begin{aligned}\int_0^{y_V} nv\,dy &= \int_0^{y_V}\left[n_0 + \frac{\epsilon}{q}\frac{dE}{dy}\right] v\,dy \\ &= n_0\int_0^{y_V} v\,dy + \frac{\epsilon}{q}\int_{E_0}^{E_V} v\,dE \\ &= n_0\left\{\left[yv - \int y\mu_0\frac{dE}{dy}\,dy\right]_0^{y_T}\right. \\ &\quad \left. + \left[yv + \int y\mu_1\frac{dE}{dy}\,dy\right]_{y_T}^{y_V}\right\} \\ &\quad + \frac{\epsilon}{q}\left\{\int_{E_0}^{E_v}\mu_0 E\,dE\right. \\ &\quad \left. + \int_{E_T}^{E_v}[v_T - \mu_1(E - E_T)]\,dE\right\}.\end{aligned}$$

Now, from (A.1), (8), and (9), one further obtains

$$\begin{aligned}\int_0^{y_V} nv\,dy &= n_0\left\{y_V v_V + \frac{1}{3}\frac{v_T - v_V}{E_V - E_T}\frac{q}{\epsilon}(n_d - n_0)y_V^2\right. \\ &\quad \left.\cdot\left(1 - \frac{\mu_1 + \mu_0}{\mu_1}\frac{y_T^3}{y_V^3}\right)\right\} \\ &\quad + \frac{\epsilon}{q}\left\{\frac{1}{2}v_T\left(E_V - \frac{E_0^2}{E_T}\right)\right. \\ &\quad \left. + \frac{1}{2}v_V(E_V - E_T)\right\}.\end{aligned}$$

Substitution of this expression into (12) and subsequent substitution of (17), (18), (11), (A.4), and (A.5) gives

$$\begin{aligned}&\frac{3}{2}\left(\frac{E_V}{E_T} - 1\right) + 2\frac{\Delta E}{E_T} \\ &= \frac{4}{3}\left(\frac{E_V}{E_T} - 1\right)\frac{1}{1 - \dfrac{v_T}{v_T - v_V}\dfrac{\Delta E}{E_T}}\left(1 + \frac{\Delta E}{E_V - E_T}\right)^2 \\ &\quad \cdot\left[1 - \frac{\mu_1 + \mu_0}{\mu_1}\left(\frac{\Delta E}{E_V - E_T + \Delta E}\right)^{3/2}\right] \\ &\quad + \frac{1}{2}\frac{v_T}{v_V}\left[\frac{E_V}{E_T} - \left(1 - \frac{\Delta E}{E_T}\right)^2\right] \\ &\quad - \frac{qD_0 n_0}{\epsilon v_V E_T}\left(\frac{v_T}{v_V} - 1\right)\left(1 - \frac{v_T}{v_T - v_V}\frac{\Delta E}{E_T}\right). \qquad \text{(C.1)}\end{aligned}$$

Keeping the assumption $\Delta E \ll E_T$ in mind, and calculating to the first order in $\Delta E/E_T$, (C.1) leads to expression (19) for the relative field drop.

Appendix D

Calculation of the Four Voltages

In this Appendix, the specific $v(E)$-characteristic given in Section II-B will be used for approximate evaluations. Now, with reference to Fig. 4 and (17), V_1 is given by

$$V_1 = LE_0 = LE_T\left(1 - \frac{\Delta E}{E_T}\right)$$

where $LE_T = 3.48$ V.

Let E_d denote the domain peak field (Fig. 4). Then V_2 can be expressed by

$$\begin{aligned}V_2 &= \frac{1}{2}L_d(E_d - E_V) \\ &= \frac{1}{2}L_d^2\frac{qn_0}{\epsilon}\left(\frac{v_T}{v_V} - 1\right)\left(1 - \frac{v_T}{v_T - v_V}\frac{\Delta E}{E_T}\right)\end{aligned}$$

where (4), (11), and (18) have been used. The numerical solutions have shown that $L_d = 2$ μm is a typical value. For $n_0 = 1.5 \times 10^{15}$ cm^{-3} V_2 is therefore approximately

$$\frac{1}{2}L_d^2\frac{qn_0}{\epsilon}\left(\frac{v_T}{v_V} - 1\right) = 6.2 \text{ V}.$$

The voltage V_3 is given by

$$V_3 = L_d(E_V - E_0) = L_d(E_V - E_T)\left(1 + \frac{\Delta E}{E_V - E_T}\right)$$

where

$$L_d(E_V - E_T) = 1.3 \text{ V}.$$

For the voltage V_4, one finds to the first order in $\Delta E/E_T$

$$V_4 = \int_0^{v_V} (E - E_0)dy = \frac{2}{3} \frac{\epsilon}{qn_0} \frac{v_V}{v_T - v_V} (E_V - E_T)^2 \cdot \left[1 + \left(\frac{v_T}{v_T - v_V} + \frac{2E_T}{E_V - E_T}\right)\frac{\Delta E}{E_T}\right]$$

where

$$\frac{2}{3} \frac{\epsilon}{qn_0} \frac{v_V}{v_T - v_V} (E_V - E_T)^2 = 0.09 \text{ V}.$$

In (22) we now substitute the expression for the four voltages, and their values suggest that for an approximate determination of L_d, (22) can be simplified to

$$LE_B = LE_T\left(1 - \frac{\Delta E}{E_T}\right) + \frac{1}{2} L_d^2 \frac{qn_0}{\epsilon}\left(\frac{v_T}{v_V} - 1\right) \cdot \left(1 - \frac{v_T}{v_T - v_V} \frac{\Delta E}{E_T}\right).$$

To the first order in $\Delta E/E_T = \Delta J/J_T$, this equation leads to expression (23) for L_d/L.

References

[1] B. S. Perlman, C. L. Upadhyayula, and W. W. Siekanowicz, "Microwave properties and applications of negative conductance transferred electron devices," *Proc. IEEE*, vol. 59, pp. 1229–1237, Aug. 1971.

[2] H. W. Thim and S. Knight, "Carrier generation and switching phenomena in n-GaAs devices," *Appl. Phys. Lett.*, vol. 11, pp. 85–87, Aug. 1967.

[3] M. P. Shaw, P. R. Solomon, and H. L. Grubin, "The influence of boundary conditions on current instabilities in GaAs," *IBM J. Res. Develop.*, vol. 13, pp. 587–590, Sept. 1969.

[4] J. Magarshack and A. Mircea, "Wideband cw amplification in X-band with Gunn diodes," in *Int. Solid-State Circuits Conf., Dig. Tech. Papers*, 1970, p. 132.

[5] ——, "Stabilization and wide band amplification using overcritically doped transferred electron diodes," in *Proc. Int. Conf. Microwave and Optical Generation and Amplification*, 1970, pp. 16. 19–16.23.

[6] H. W. Thim, "Experimental verification of bistable switching with Gunn diodes," *Electron. Lett.*, vol. 7, pp. 246–247, May 1971.

[7] D. Boccon-Gibod and J. L. Teszner, "Experimental evidence of bistable switching in a Gunn epitaxial coplanar diode by anode-surface loading," *Electron. Lett.*, vol. 7, pp. 468–469, Aug. 1971.

[8] P. Guéret, "Convective and absolute instabilities in semiconductors exhibiting negative differential mobility," *Phys. Rev. Lett.*, vol. 27, pp. 256–259, Aug. 1971.

[9] H. W. Thim, "Stability and switching in overcritically doped Gunn diodes," *Proc. IEEE* (Lett.), vol. 59, pp. 1285–1286, Aug. 1971.

[10] P. Guéret and M. Reiser, "Switching behavior of over-critically doped Gunn diodes," *Appl. Phys. Lett.*, vol. 20, pp. 60–62, Jan. 1972.

[11] P. Jeppesen and B. Jeppsson, "The influence of diffusion on the stability of the supercritical transferred electron amplifier," *Proc. IEEE* (Lett.), vol. 60, pp. 452–454, Apr. 1972.

[12] H. L. Grubin, M. P. Shaw, and E. M. Conwell, "Current instabilities in n-InP," *Appl. Phys. Lett.*, vol. 18, pp. 211–213, Mar. 1971.

[13] J. A. Copeland and S. Knight, "Applications utilizing bulk negative resistance," in *Semiconductors and Semimetals*, vol. 7A, R. K. Willardson and A. C. Beer, Ed. New York: Academic, 1971, pp. 3–72.

[14] F. Sterzer, "Stabilization of supercritical transferred-electron amplifiers," *Proc. IEEE* (Lett.), vol. 57, pp. 1781–1783, Oct. 1969.

[15] W. Shockley, "Negative resistance arising from transit time in semiconductor diodes," *Bell Syst. Tech. J.*, vol. 33, pp. 799–826, July 1954.

[16] P. S. Hauge, "Static negative resistance in Gunn effect materials with field-dependent carrier diffusion," *IEEE Trans. Electron Devices* (Corresp.), vol. ED-18, pp. 390–391, June 1971.

[17] G. Döhler, "Shockley's positive conductance theorem for Gunn materials with field-dependent diffusion," *IEEE Trans. Electron Devices* (Corresp.), vol. ED-18, pp. 1190–1192, Dec. 1971.